Growth of fruiting bodies was initiated by mycelial cells, which divided to form a group of cells between the leaf surface and the mycelia. These cells grew radially and the marginal cells bifurcated, thus increasing the number of radiating rows of cells as the fruiting bodies grew in diameter (Fig. 5). No well-defined ostioles were present, but at maturity fissures developed radially in the fruiting bodies and groups of cells often broke away from the center (Fig. 7), allowing the spores to escape.

Two distinct groups of fruiting bodies can be distinguished in this form of *Asterina* on the basis of size. In one group the diameter of the fruiting bodies ranges from 36 to 42 microns; in the other group (Fig. 7) (in which ascospores have been found) it ranges from 100 to 210 microns. No pycnidiospores were found in association with the smaller fruiting bodies, although several of the smaller bodies had split open and hence were mature. In modern forms of *Asterina* pycnidia identical with mature ascocarps, except for their diminutive size, are present (*5*). Hence the smaller fruiting bodies of the fossil may be pycnidia. Thus both asexual fruiting bodies (pycnidia) and sexual fruiting bodies (ascocarps) are present in this fossil form of *Asterina.*

As this study continues several presently little known or unknown fungi will be added to the fossil record. As various morphological forms of the life cycles of these fossil epiphyllous fungi are found they and their often isolated parts can better be related to the modern groups to which they belong. Because of the preliminary nature of this report, species names have not been assigned to these fossils (*6*).

Meliola and *Asterina* are presently distributed around the world but are most abundant in warm, humid areas. Thus this discovery of these two genera supports the theory proposed by E. W. Berry (*7*) that the vegetation of the Mississippi embayment in Tennessee during the Eocene reflects the influences of a humid, subtropical climate.

DAVID L. DILCHER

Department of Biology, Yale University, New Haven, Connecticut

References and Notes

1. C. Köck, *Deutsch. Akad. Naturforscher Nova Acta N. F.* **6**, 333 (1939).
2. W. N. Edwards, *Trans. Brit. Mycol. Soc.* **8**, 66 (1922).
3. I. C. Cookson, *Proc. Linnean Soc. New South Wales* **72**, 207 (1947).
4. C. G. Hansford, *Sydovia Ann. Micol. Ser. II*, suppl. 2, (1961).
5. E. M. Doidge, *Trans. Roy. Soc. South Africa* **8**, 235 (1920).
6. A comprehensive report is in preparation.
7. E. W. Berry, *U.S. Geol. Surv. Profess. Paper 156* (1930), pp. 33–40.

5 August 1963

Equatorial Undercurrent and Related Currents off Brazil in March and April 1963

Abstract. *In 1963, the source of the Equatorial Undercurrent appeared to be near 38°W. This undercurrent was an equatorial extension of a narrow saline current setting east-southeast at the surface near 2°N 42°W. Near 38°W, a retroverse branch of the Guiana Current also joined the Equatorial Undercurrent. Surface flow was easterly along all of the east-southeast current and the undercurrent observed. The subsurface-velocity maximum of the undercurrent was higher at 35°W than at 38°W.*

Observations taken off northeastern Brazil during March and April 1963 (*1*) indicate the westernmost position of the Equatorial Undercurrent on the Equator in its typical form and clearly delineate the currents which lead to that location. These observations, consisting primarily of closely spaced measurements of temperature and salinity and measurements of current on the Equator by means of parachute drogues (*2*), were apparently the first specifically designed for the investigation of the Equatorial Undercurrent and related currents off Brazil. Many valuable confirmations were provided from the less accurate indications of current by departures from dead reckoning and by the behavior of the hydrographic wire.

Among the distinguishing characteristics of the Equatorial Undercurrent in the Atlantic listed by Metcalf *et al.* (*3*) and by Montgomery (*4*) are a subsurface eastward velocity maximum and a high maximum salinity (near the velocity maximum) in the upper thermocline very close to the Equator. These characteristics were observed in 1963 as far west as 37°W (see Figs. 1 and 2) and existed probably up to 38° or 39°W. But at 40°W, the drogues showed a surface current of 2.7 km/hr (1.5 knot) west-northwest, the Guiana Current, and virtually no current at 100-m depth. However, eastward flow may have been present below 100 m. At 42°W, the slopes of isosteres in the vertical section (Fig. 3) do not show that the Equatorial Undercurrent was present on the Equator, and the maneuvering necessary to maintain a small wire angle at the station on the Equator indicated a surface current to the northwest, the Guiana Current.

The Equatorial Undercurrent appeared as an extension of a surface current setting mainly east-southeast, which entered the region of observation between 1° and 3°N, as Fig. 1 shows. Since it has no appropriate name, this current will be referred to as the ESE current. At the westernmost line, it is clearly indicated to depths exceeding 300 m from the slope of isosteres given in Fig. 3. The current was characterized by a high salinity maximum (Fig. 2) between 60 and 90 m where the water temperature was 22.5° to 25.5°C. To the south, it was separated from the Guiana Current by a small region of low maximum salinity. To the north, the northern branch of the South Equatorial Current was distinguished by low maximum salinity.

Neumann's (*5*) chart of geostrophic surface currents shows the ESE current. The chart is based on data taken at all seasons over a period of many years until 1946. Such a chart may be subject to question, but it is in good agreement with the *Laserre* observations (*1*).

The maximum salinities (Fig. 2) indicate that a retroverse branch of the Guiana Current joined the Equatorial Undercurrent near 38°W. The high salinity region, near 40°W broadened, apparently at the turn of the current. The salinity maximum at 37°W was higher than that in the ESE current. Thus the tongue of high salinity between 40° and 35°W evidently came from the south. The tongue was not centered on the Equator, but close to 1°S, apparently because the water of the Guiana Current remained on the south side of the stream. Preliminary topography of the isosteric surface of 200 centiliters per metric ton suggests a turn in the geostrophic current in agreement with that inferred from the maximum salinity distribution.

It is noteworthy that the turns in both the ESE current and the branch of the Guiana Current were found quite near the Equator.

Easterly surface flow was observed in

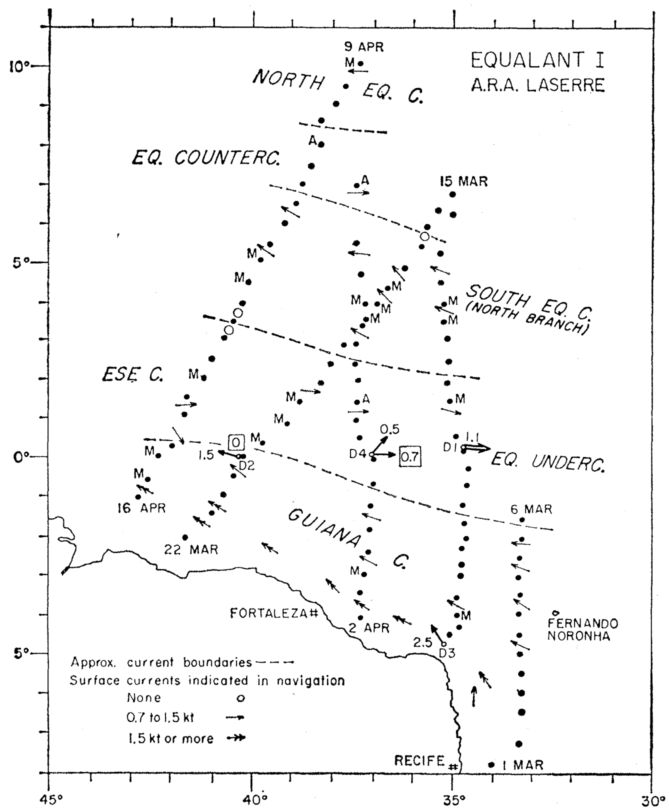

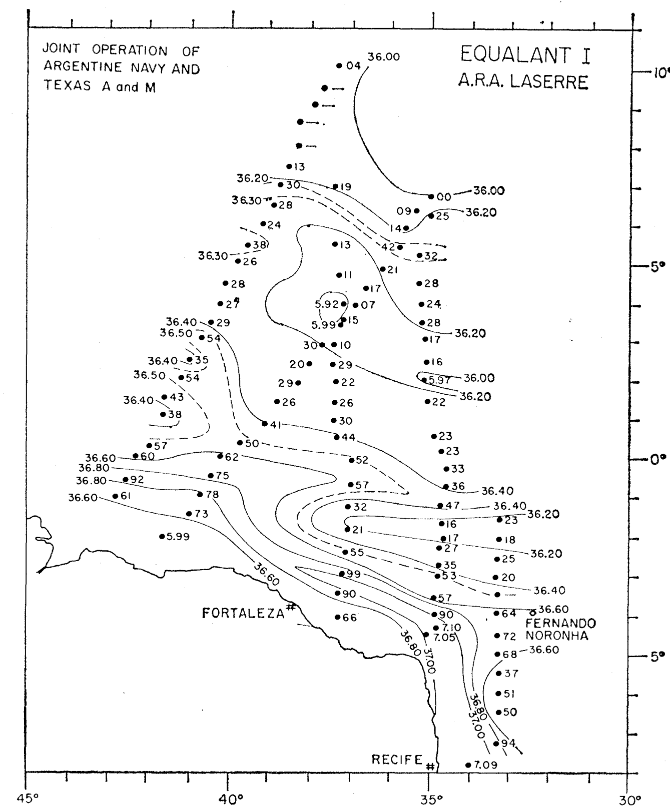

Fig. 1 (left). Current in knots (1 knot = 1.85 km/hr) indicated by drogues, designated by *D* and by departure from dead reckoning. Speed at 100 m is indicated in a box. Shear between the surface and 100 m is indicated by an open arrow. Locations are shown where the current of each region was clearly indicated by maneuvering needed to reduce wire angle (*M*) or by horizontal or vertical wire angle (*A*). Fig. 2 (right). Maximum observed subsurface salinity in per millage, abbreviated by dropping 36 or the 3 in 35 or 37 per mil. Dash indicates a surface maximum.

both the ESE current and the Equatorial Undercurrent wherever these currents were crossed during the cruise. Drogues within the undercurrent suggest that there was a downstream increase in speed near the subsurface salinity maximum, leading to the typical marked subsurface speed maximum observed at 35°W.

At 37°W on the Equator, the velocity at 100 m was only a little higher than that at the surface, as Fig. 1 shows. But at 35°W (0.5°N) the velocity at 100 m was 2.7 km/hr (1.5 knot (east) greater than at the surface, where the current was roughly 0.9 km/hr east. Interestingly, the wind near the drogue station at 35°N was quite weak.

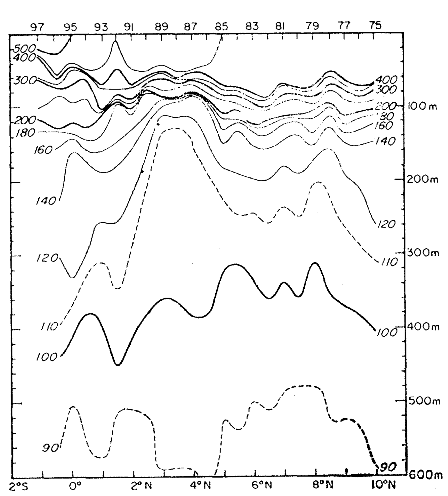

Fig. 3. Thermosteric anomaly in centiliters per metric for the westernmost line of observations.

The Equatorial Countercurrent was present as a band of weak easterly flow between 6.5° and 8.5°N characterized by relatively high maximum salinity, as shown in Figs. 1, 2, and 3.

The results raise the question of the origin of the ESE current. Neumann's (*5*) chart of geostrophic currents shows the current extending to the region where it was observed in March and April 1963 from the northwest, passing 50°W at about 7°N. Near there, according to current charts based on departures from dead reckoning, such as the United States Navy Hydrographic Office Provisional Charts of the Tropical Atlantic (*6*), easterly sets prevail even in winter and early spring. A line of maximum salinities exceeding 36.5 per mil about 480 km (300 miles) off Brazil which is shown by Metcalf *et al.* (*3*, Fig. 10) appears to follow the path of the ESE current given by Neumann (*5*).

It is not clear whether the bulk of the ESE current comes primarily from one or more retroverse branches of the Guiana Current or from the Equatorial Countercurrent and its relatives. Possibly the ESE current and the Equatorial Countercurrent constitute two branches from a common easterly flow centered near 7°N, 50°W. Association between the two currents is suggested by the narrow, indistinct separation between them (Fig. 3) from 300 m to 450 m. According to Montgomery (*4*), there is close association between the Equatorial Countercurrent and the Equatorial Undercurrent in the western Pacific.

JOHN D. COCHRANE

Department of Oceanography and Meteorology, Agricultural and Mechanical College of Texas, College Station

References and Notes

1. The observations were jointly made by the Argentine Navy Hydrographic Service and the Department of Oceanography of the Texas A and M College as a part of the Equalant I Operation of the International Cooperative Investigation of the Tropical Atlantic. The work was done aboard the Argentine Navy Ship *Comodoro Laserre* under command of

Capt. de Corb. H. J. Gomez Beret. The portion by Texas A and M was supported by contract Nonr 2119 (04) with the Office of Naval Research.

2. Currents were measured by steaming a number of times between the drogue and a reference buoy. Measurement of speeds involved estimates of ship's speed from normal engine turning rates and are therefore not notably accurate although directions and relative magnitudes are reliable. For discussion of drogues see G. Volkmann, J. Knouss, A. Vine, *Trans. Amer. Geophys. Union* **37**, 573 (1956).
3. W. G. Metcalf *et al.*, *J. Geophys. Res.* **67**, 2499 (1962).
4. R. B. Montgomery, *J. Oceanogr. Soc. Japan*, 20th Anniversary Volume, 487 (1962).
5. G. Neumann, *Deep-Sea Res.* **6**, 328 (1960).
6. *Provisional Oceanographic Charts of the Tropical Atlantic Ocean* (U.S. Navy Hydrographic Office, Washington 25, D.C., 1962).

22 July 1963

Infrared Emissivity of the Sahara from Tiros Data

Abstract. *Most rocks, minerals, and sands show strong infrared reflection bands. In the atmospheric window (8 to 12μ), quartz and feldspar show an emissivity near 0.8, calcite near 1.0. These laboratory data are confirmed from observations during a Tiros flight over the Libyan desert. The Mediterranean Sea was used for calibration. Desert emissivity is between 0.7 and 0.9.*

Signals received in the 8- to 12-μ water vapor "window" radiation channel of Tiros weather satellite depend on atmospheric emission and absorption, surface temperature, and vertical surface emissivity and reflectivity in the wavelengths concerned. Vertical emissivity, ϵ, is the ratio of the vertically emitted radiant power from a source to that from a blackbody at the same temperature (and at the same wavelength). Therefore, the emissivity of a blackbody is unity. For opaque materials the verticale reflectivity is (1-ϵ). For clear air the atmospheric effect can be calculated (*1*). In the following example the atmospheric effect can be circumvented and deductions made about the emissivity of the desert surface.

Let ϵ_λ be the vertical emissivity at wavelength λ. Other subscripts refer to certain broad wavelength bands: ϵ_t = total coefficient at a certain temperature, ϵ_w for the water vapor window at 8 to 12 μ. Some data in the far infrared can be directly or indirectly evaluated from literature. Sand (*2*) of the Baltic shore has $\epsilon_t = 0.89$ at 300°K. The main constituent here seems to be quartz which has very low emission around 9 μ. This would then result in ϵ_w being close to 0.8. Similar data are found for granite, quartz, basalt, gabbro, and many other igneous rocks (*3*). Our own data show the same for feldspar.

On the other hand, water (*4*), ice, snow (*2*), vegetation, calcite, marble, and limestone (*5*), indicate $\epsilon_w > 0.95$. The emissivities for different rocks and minerals show quite complicated spectral curves. Minima of ϵ_λ for quartz and feldspar lie in the 10-μ window, but those of calcite are outside the window (*5*).

Most older meteorological literature does not consider a deviation of ϵ_t or ϵ_w from unity. The advanced state of infrared reconnaissance and the satellites demonstrates the painful lack of knowledge of ϵ data. Evaluation of infrared signals may depend more on ϵ than on temperature. At noon with the sun shining brightly a dry sand has a lower ϵ_w and a higher temperature than an adjacent wet sand. The signal from dry sand may be higher or lower than that of the wet sand depending on whether the change of ϵ or that of the temperature is more important.

The published data for ϵ_w or ϵ_t which are much lower than 0.8 seem to be erroneous: snow, 0.35 (*6*); terrain, 0.35 (*7*); gravel, plowed field and granite, 0.28 to 0.44 (*8*).

Confirmation of these statements can be found from Tiros III window observations, if proper evaluation of instrumental and atmospheric influences can be made. This has been done for orbit 44, 8 to 12 μ, 15 July 1961, 1042 to 1055 UT, a flight which has been discussed by Nordberg *et al.* (*9*). This passage covered two important areas, the Mediterranean Sea north of Libya, and the Libyan and Egyptian desert roughly between latitudes 20° and 30° N and longitudes 20° and 30° E. This desert area is known as one of the ideal deserts, free of vegetation, surface water, and people. Oases (Cufra, Siva) cover minute areas, elevations are below 400 m. On the day of this flight both areas were in, or to the east of, a weak anticyclone. No clouds were reported by ground observers or Tiros. A uniform light northerly wind had been blowing at the area for 36 hours prior to the observation. The average shelter temperature of 12 stations in the desert area (at 1300 local time) was 38°C, a figure coinciding with the average July maximum for this area (*10*).

Longer and shorter series of observations of surface versus shelter temperatures exist for about six Sahara stations (*10*, *11*). Surfaces consist of either sand or fine gravel in dry wadis. The average temperature difference in July between surface and air is 20° to 32°C at 1300 local time. The winds for this area are usually quite weak, so that it is likely the higher temperature difference might apply. On the other hand, part of the area is covered by horizontally stratified rock for which the difference might be as low as 10°C. The surface temperature, then, might be between 48° and 70°C. The air mass over the Sahara comes from the Mediterranean; hence, no water vapor could be added or subtracted to the air of this trajectory. Therefore, the attenuation of the surface radiation is almost equal over sea and land.

Water, CO_2, and O_3 vapors emit radiation to Tiros. Again, the emitted radiation was equal over land and sea for heights above 500 to 1000 m. Below this level all air layers are warmer over land and emit more. A portion $(1-\epsilon_w)$ of the atmospheric emission will be reflected by the surface and received in a somewhat attenuated form by Tiros. Effects in this paragraph would lower the computed ϵ_w even more, but they probably are small.

Therefore, we expect the Tiros record to change by an amount equivalent to a surface temperature difference of 18° to 40°C when going from sea to land. Actually, the equivalent of an 11°C change (from 288° to 299°K) was recorded by Tiros. Assuming equal atmospheric influences over sea and desert, we can from this deviation derive ϵ_w (desert) if ϵ_w (sea) is known. The ϵ_w (sea) is 0.98 for clean water (*5*) and 0.96 for water with a very thin oil layer on it (*12*). When ϵ_w (sea) = 0.98 we find ϵ_w (desert) between 0.69 and 0.91.

KONRAD J. K. BUETTNER
CLIFFORD D. KERN
Department of Atomospheric Sciences, University of Washington, Seattle 5

References

1. S. M. Greenfield and W. W. Kellogg, *J. Meteorol.* **17**, 283 (1960).
2. G. Falkenberg, *Meteorol. Z.* **45**, 334 (1928).
3. R. J. Lyon and E. A. Burns, *Econ. Geol.* **58**, 274 (1963).
4. J. Lecomte, "Spectroscopic dans l'infrarouge," in *Handbuch der Physik* (Springer, Berlin, 1958), vol. 26, p. 2
5. K. J. K. Buettner and C. D. Kern, in preparation.
6. C. D. Miller, in *Proceedings of the Second Symposium on Remote Sensing of the Environment* (Univ. of Michigan, Ann Arbor, 1963).
7. P. Kruse, L. McGlauchlin, R. McQuistan,